Methods and Applications

Evaluation of Measles Vaccine Immunogenicity and Durability Using A Pseudotyped Virus Neutralization Assay

Qi Jiang'; Xi Wu'; Jie Zhang'; Huiling Wang²; Fangyu Dong³; Xuelian Wu'; Pengju Yu'; Jianhui Nie'; Youchun Wang⁴; Weijin Huang¹; Jiuyue Zhou³; Yaru Quan⁵; Yan Zhang²-♯; Suting Wang⁶-♯; Juan Li⁵-♯

ABSTRACT

Introduction: This study aimed to establish a robust method for monitoring measles vaccine-induced immunity and assessing population-level serostatus.

Methods: This study constructed a vesicular stomatitis virus (VSV)-based pseudotyped virus system expressing envelope proteins from seven major circulating measles genotypes (H1, B3, D4, D8, D9, D11, G3) and the Schwarz vaccine strain (genotype A), thereby enabling a high-throughput neutralization assay for antibody detection.

Results: Vaccination induced a substantial increase in neutralizing antibody geometric mean titers (GMT) post-immunization (4,808 after the first dose; 5,326 after the second dose), with antibody levels remaining elevated in 4-year-old children (GMT: 3,834). Crossneutralization activity against different genotypes varied by less than 6.4-fold, demonstrating broad protective immunity. However, 12% of adult sera tested were seronegative, revealing the presence of susceptible populations.

Conclusions: This study confirms the robust immunogenicity of the current measles vaccine and establishes a valuable tool for serosurveillance and long-term immunity assessment.

Measles virus (MeV) is a highly contagious pathogen that spreads rapidly through airborne transmission, with a basic reproduction number (R0) ranging from 12 to 18. Consequently, localized outbreaks or large-scale epidemics can emerge when the proportion of susceptible individuals exceeds 10%. Prior to the introduction of measles vaccination, the virus caused millions of deaths worldwide each year (1).

The Edmonston wild-type strain, isolated in 1954, serves as the ancestral virus for the measles vaccine used globally. The first-generation measles attenuated

vaccine (Edmonston strain B) derived from this strain received approval in the United States in 1963. Despite the availability of a safe and effective measles vaccine for decades and global immunization programs achieving approximately 86% coverage among target populations, measles remains a leading cause of childhood mortality worldwide, particularly among children under five years of age (2). Using measles case data reported by countries to the World Health Organization (WHO) and the United Nations Children's Fund (UNICEF), the research team led by Anna A. Minta and Matt Ferrari developed an estimation model for measles cases and deaths. According to their model, the estimated annual number of measles deaths declined from 800,000 in 2000 to 107,500 in 2023, representing an 87% reduction. However, in recent years, factors including the coronavirus disease 2019 (COVID-19) pandemic, economic instability, natural disasters, famine, and population displacement have caused stagnation or declines in routine and supplementary immunization coverage, resulting in a continuous increase in measles cases (3). According to the latest data from the WHO and the U.S. CDC, an estimated 10.3 million measles cases occurred globally in 2023, representing a 20% increase compared to 2022, with approximately 108,000 associated deaths. Outbreaks were reported in all WHO regions except the Americas, with nearly half of the cases occurring in Africa. From March 1, 2024, to February 28, 2025, a total of 28,791 measles cases were reported in the European Union, with 86% occurring in unvaccinated individuals. Between January 1 and March 20, 2025, the United States reported 378 measles cases, with at least 75% occurring in unvaccinated individuals (4).

Measles eradication depends on achieving and maintaining high vaccination coverage to sustain herd immunity. Consequently, continuous surveillance of population-level measles antibody titers, coupled with timely supplementary and booster vaccination of unvaccinated or susceptible individuals, is critically

important. However, conventional enzyme-linked immunosorbent assays (ELISA) suffer from limited specificity and susceptibility to environmental interference, whereas plaque reduction neutralization tests (PRNT) are constrained by low throughput and extended testing durations (5). To overcome these limitations, we developed a reliable, stable, rapid, and highly specific pseudotyped virus-based in vitro neutralization assay for detecting measles-neutralizing This method complements existing antibodies. serological assays and was applied to evaluate population immunity levels and assess both the immunogenicity and durability of the current measles vaccine.

METHODS

Plasmids, Sera, and Cells

The hemagglutinin (H) protein (GenBank: AAA56657.1) and fusion (F) protein (GenBank: AAA56656.1) genes from the measles virus (MeV) vaccine strain Schwarz, together with the H and F gene sequences from seven circulating strains — B3 (KT732216.1), D4 (JN635402.1), D8 (KT732231.1), (KY969476.1), D11 (MN017369.1), (KC164758.1), and H1 (ON035899.1) — as well as one sequenced virus isolate, were codon-optimized and individually cloned into the pcDNA3.1 vector. This cloning strategy generated the pcDNA3.1-H and pcDNA3.1-F expression constructs, respectively (Supplementary Figure S1, available at https://weekly. chinacdc.cn/).

A total of 42 serum samples were collected from infants and young children at four time points: before measles-mumps-rubella (MMR) vaccination, after the first dose, after the second dose, and at 4 years of age. These samples were obtained through the Shandong CDC. Additionally, 50 adult serum samples were collected from Shandong Taibang Biological Products Co., Ltd. All samples were collected under protocols ensuring donor safety and maintaining complete anonymization of personal identifying information.

Mouse sera were collected at week 6 following an immunization regimen that consisted of an initial dose of MeV H protein DNA vaccine, followed by two booster immunizations with measles pseudotyped virus administered at two-week intervals.

Twenty-one cell lines were cultured for this study: HEK 293T, MRC5, A549, HeLa, SK-N-MC, Hep2, HepG2, Huh7, Vero, LLC-MK2, CHO, BHK21,

NIH3T3, MDCK, Cf2TH, Mv1Lu, PK15, MDBK, CRFK, and Vero-SLAM. All cells were maintained in Dulbecco's Modified Eagle Medium (DMEM) or the manufacturer-recommended medium supplemented with 100 U/mL penicillin-streptomycin (GIBCO) and 10% fetal bovine serum (FBS; Pansera ES, PAN-Biotech) at 37 °C in a humidified atmosphere containing 5% CO₂.

HEK 293T cells were stably transfected with NECTIN4 and SLAM receptor genes to generate stable cell lines designated 293T-NECTIN4 and 293T-SLAM, respectively. These cell lines were established through antibiotic selection using 1.5 mg/L puromycin and 150 mg/L hygromycin B, respectively.

Pseudotyped Virus Packaging

HEK 293T cells were transfected with a mixture of pcDNA3.1-H and pcDNA3.1-F plasmids at a 4:1 ratio using the Lipofectamine 3000 Transfection Kit (Invitrogen, USA) following the manufacturer's protocol. Six hours post-transfection, cells were infected with 6-9G* Δ G-GFP VSV pseudotyped virus for 4 hours. Culture supernatants containing pseudotyped virus were harvested 24 hours post-infection and clarified by centrifugation at 4,000 ×g for 10 minutes at 4 °C. The clarified supernatants were then filtered through 0.45 μ m sterile membranes, aliquoted, and stored at -80 °C until use.

Pseudotyped Virus Titration

Serial 3-fold dilutions of MeV-GFP pseudotyped virus stock (50 μL per well) were prepared in 96-well clear cell-culture plates. Each well received 100 μL of 293T-NECTIN4 cell suspension (4×10⁵ cells/mL), and plates were incubated for 24 hours at 37 °C in a humidified atmosphere containing 5% CO₂. GFP-positive cells were enumerated using a fluorescence cell counter (Cytation 5, BioTek), and viral titers were expressed as focus-forming units per milliliter (FFU/mL).

Pseudotyped Virus Neutralization

Samples were initially diluted 1:30 in 96-well plates, followed by 3-fold serial dilutions. MeV-GFP pseudotyped virus was added at a multiplicity of infection (MOI) of 1.4, and the mixture was incubated at 37 °C with 5% $\rm CO_2$ for 1 hour. Subsequently, 100 $\rm \mu L$ of 293T-NECTIN4 cell suspension (4×10⁵ cells/mL) was added to each well, and plates were incubated for 24 hours at 37 °C with 5% $\rm CO_2$. GFP-

positive cells were quantified using a BioTek fluorescence reader. The 50% neutralization titer (NT $_{50}$) was calculated using the Reed-Muench method to determine neutralizing antibody levels in the samples (6).

Microneutralization Experiments

The 25 μ L serum sample was subjected to 2-fold serial dilution in 96-well microplates and were mixed with 25 μ L of 100 TCID $_{50}$ measles virus. The mixture was incubated at 37 °C with 5% CO $_2$ for 90 minutes. Subsequently, 100 μ L of Vero-SLAM cell suspension at a density of 1–1.5 × 10 5 cells/mL was added to each well. Plates were incubated at 37 °C with 5% CO $_2$ for 2 to 5 days (typically 3 days) to monitor cytopathic effects (CPE). The antibody titer was defined as the highest serum dilution that completely inhibited CPE.

RESULTS

Selection of Viral Strains

We retrieved representative circulating measles virus genotypes (B3, D4, D8, D9, D11, G3, H1) from the MeaNS database based on recent epidemiological surveillance data. These strains, together with the vaccine strain (genotype A), underwent nucleotide sequence analysis of the hemagglutinin (H) gene to construct a phylogenetic tree and assess genetic

distances. Following screening for strains with complete H and F protein sequences, we generated pseudotyped viruses representing eight distinct genotypes. Amino acid sequence analysis of the H protein revealed that the phylogenetic tree clustered into nine distinct groups (Supplementary Figure S2A, available at https://weekly.chinacdc.cn/). The eight representative strains selected exhibited H protein sequences of 618 amino acid residues with 93.53% to 98.22% identity (Supplementary Figure S2).

NECTIN4 and SLAM Receptors Enhance Measles Virus Infectivity

To evaluate receptor-dependent infectivity, we challenged 21 cell lines derived from eight host species with the MeV pseudotyped virus (genotype H1). These included 10 human, 2 monkey, 3 mouse, and 2 canine cell lines, as well as one each from mink, pig, cattle, and cat origins. Among these, two cell lines stably overexpressing receptors — 293T-NECTIN4 and 293T-SLAM — were included for comparison. As shown in Figure 1, the MeV pseudotyped virus failed to infect parental 293T cells but efficiently infected 293T-NECTIN4 and 293T-SLAM cells. Infection of other cell lines was either minimal or absent, demonstrating that NECTIN4 and SLAM receptors are essential for MeV pseudotyped virus entry. Since 293T-NECTIN4 cells exhibited the highest infection rate, this cell line was selected for all

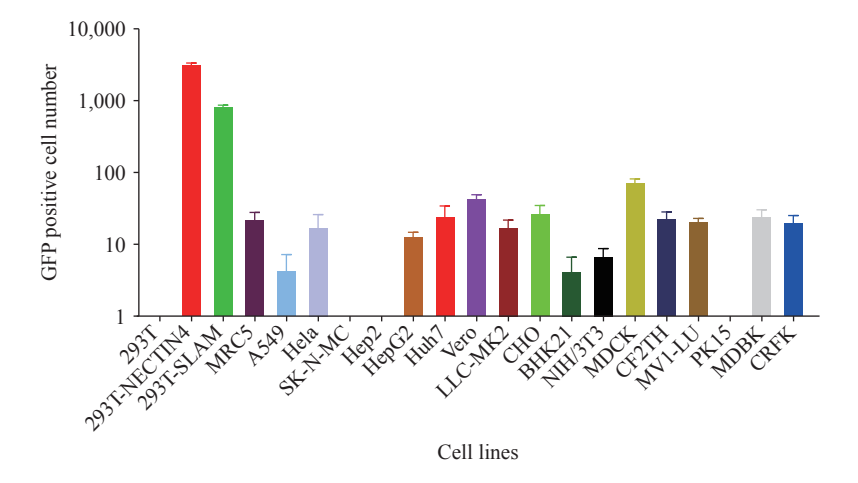


FIGURE 1. Infectivity of measles pseudotyped virus in different cell lines. Abbreviation: 293T=human embryonic kidney cells; 293T-NECTIN4=human embryonic kidney cells expressing NECTIN4; 293T- SLAM=human embryonic kidney cells expressing SLAM; MRC5=human lung fibroblast cells; A549=human lung cancer cells; HeLa=human cervical cancer cells; SK-N-MC=human neuroblastoma cell line; Hep2=human larynx epidermal carcinoma cell line; HepG2=human hepatocellular carcinoma cells; Huh-7=human hepatocellular carcinoma cells; Vero=African green monkey kidney cells; LLC-MK2=Rhesus monkey kidney cells; CHO=Chinese hamster ovary cells; BHK21=baby hamster kidney cells; NIH-3T3=mouse embryo fibroblast cells; MDCK=canine kidney cells; CF2TH=canine thymus cells; MV1-LU=mink cell line; PK15=pig kidney cell line; MDBK=bovine kidney cells.

subsequent pseudotyped virus experiments (Figure 1).

The x-axis indicates the different cell lines tested, and the y-axis represents the log₁₀ number of GFP-positive cells produced following incubation with the measles virus pseudotyped virus.

Establishment and Validation of the Pseudotyped Virus Neutralization Assay

To establish a robust in vitro neutralization assay using measles pseudotyped virus, we systematically optimized key assay parameters, including cell seeding density $(1.6 \times 10^2 \text{ to } 3.2 \times 10^5 \text{ cells/well})$, pseudotyped virus input (MOI ranging from 0.017 to 114), and incubation duration (8 to 120 hours). Our results demonstrated that the number of GFP-positive cells increased proportionally with higher cell seeding densities. NT₅₀ remained stable across the cell density range of 1.6×10² to 4×10⁴ cells/well, with linear correlation coefficients (R²) consistently exceeding 0.995 within the 1.3×10^3 to 4×10^4 cells/well range. Based on these findings, we selected 4×10⁴ cells/well as the optimal cell density for subsequent assays (Figure 2A and 2B). When the pseudotyped virus MOI ranged from 0.017 to 1.4, NT₅₀ values remained stable, achieving an R² of 0.998 at MOI=1.4. Consequently, an MOI of 1.4 was chosen for all further experiments (Figure 2C). GFP-positive cell counts increased with extended incubation time and reached a plateau after 60 hours. NT₅₀ values remained stable between 12 and 120 hours, with R² values exceeding 0.999 during the 24- to 60-hour window. To optimize the balance between assay accuracy and time efficiency, we selected a 24-hour post-infection incubation period as the optimal detection time (Figure 2D and 2E).

To validate the assay's reliability, we systematically evaluated multiple performance parameters: cut-off value, specificity, linearity, dynamic range, robustness, precision, and correlation with the authentic virus neutralization test. The cut-off value was established at 150, derived from the mean plus three standard deviations (mean + 3SD=154) of negative serum samples (Figure 2F). Measles antibody-positive sera exclusively exhibited neutralizing activity against the measles pseudotyped virus, confirming high assay specificity (Figure 2G). Within an inhibition range of 20% to 90%, the assay demonstrated a robust linear relationship between sample dilution and response (R²>0.92) (Figures 2H and 2I). We further validated the method's robustness by systematically varying

experimental conditions: incubation time of the pseudovirus from 0.5 h to 1.5 h (Figure 2]), different batches of pseudovirus (Figure 2K), 1 to 3 freeze-thaw cycles of the pseudovirus (Figure 2L), and 1 to 3 freeze-thaw cycles of the serum samples (Figure 2M). For each condition, three serum samples were subjected to three independent experiments, with six replicates per experiment. Minor variations in experimental parameters resulted in NT₅₀ values within a twofold range, confirming excellent assay robustness. Repeated measurements of identical samples yielded intra-assay coefficients of variation (CV) ranging from 6.1% to 19.8% and inter-assay CVs between 10.6% and 17.1%, demonstrating strong assay precision (Figure 2N). Finally, correlation analysis of 42 serum samples tested by both the pseudotyped virus assay and the authentic virus microneutralization test revealed a strong positive correlation (y=0.756x+1.852, r=0.85), confirming excellent agreement between the two methods.

Cross-protection by Antibodies Against Different Genotypes of Measles Virus

To assess the potential for immune escape among different measles virus strains, we selected genotypes H1 and B3 for animal immunization and performed neutralization assays using pseudotyped viruses representing eight measles virus genotypes with the corresponding immunized mouse sera. Sera from H1immunized mice exhibited average neutralizing antibody titers (NT₅₀) against genotypes A, H1, B3, D4, D8, D9, D11, and G3 of 2,863; 18,316; 7,286; 12,570; 8,602; 6,011; 4,004; and 12,378, respectively. from B3-immunized mice demonstrated corresponding NT₅₀ values of 4,437; 12,227; 17,525; 16,234; 14,155; 11,923; 5,693; and 16,182, respectively. Notably, the variation in neutralization titers across different genotypes did not exceed 6.4fold. Given that all antibody titers remained substantially above the protection threshold, current vaccines provide full protection against diverse circulating strains (Figure 3).

Vaccine Evaluation

To assess the immunogenicity, durability, and cross-protective efficacy of the measles vaccine against various genotypes, we performed neutralization assays using sera collected from 42 individuals at four time points: pre-vaccination (8 months of age), after the first dose of MMR vaccine, after the second dose, and

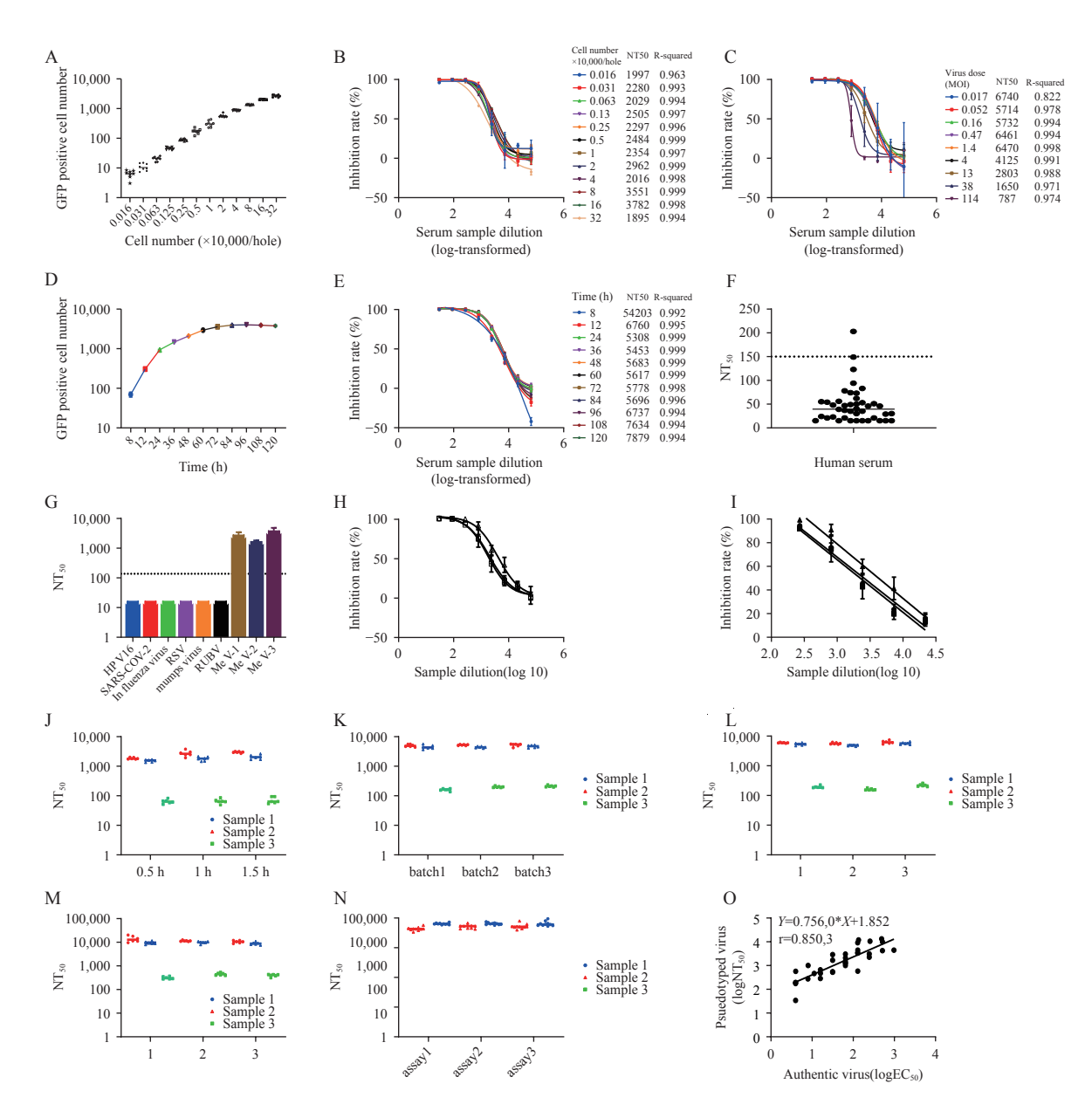


FIGURE 2. Establishment and validation of an in vitro neutralizing antibody detection method based on measles pseudotyped virus. (A) Effect of varying cell seeding densities on measles pseudotyped virus titration; (B) Effect of different cell seeding densities on measles pseudotyped virus neutralization; (C) Effect of varying pseudotyped virus input amounts on neutralization; (D) Effect of different incubation times on measles pseudotyped virus titration; (E) Effect of different incubation times on neutralizing antibody detection using the measles pseudotyped virus assay; (F) Determination of the cut-off value for the in vitro neutralizing antibody assay; (G) Specificity validation of the neutralization assay; (H) Linear range assessment of the neutralizing antibody assay; (I) Linearity assessment of the neutralizing antibody assay. Robustness of the assay under varying experimental conditions: (J) incubation time of the pseudovirus varied from 0.5 to 1.5 hours; (K) different batches of pseudovirus were used; (L) pseudovirus underwent 1 to 3 freeze—thaw cycles; (M) serum samples underwent 1 to 3 freeze—thaw cycles; (N) Precision assessment of the neutralizing antibody assay; (O) Correlation between the pseudotyped virus neutralization assay developed in this study and the gold-standard live virus neutralization assay.

Note: For (M), 3 serum samples were subjected to three independent experiments, with 6 replicates per experiment.

at 4 years of age. The geometric mean neutralizing antibody titers (NT_{50}) were 48, 4,808, 5,326, and 3,834, respectively. Compared to pre-vaccination sera, antibody levels increased approximately 100-fold after

the first dose, 110-fold after the second dose, and remained 80-fold higher at 4 years, demonstrating robust immunogenicity and sustained immunity. Student's *t*-test was performed to examine sex-based

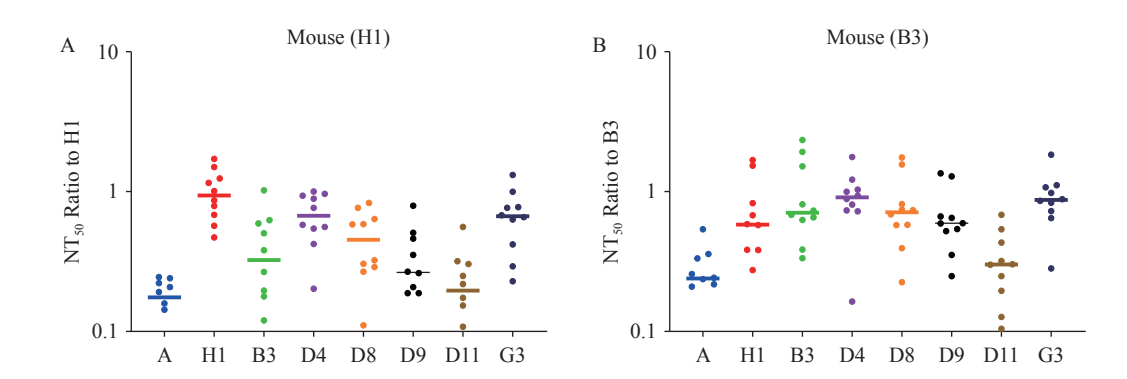


FIGURE 3. Cross-neutralization of measles pseudotyped virus. (A) Neutralization assay of measles pseudotyped viruses representing different genotypes using sera from mice immunized with the H1 genotype. (B) Neutralization assay of measles pseudotyped viruses representing different genotypes using sera from mice immunized with the B3 genotype. Note: For (A), the x-axis indicates the various measles pseudotyped virus genotypes, and the y-axis shows the fold change in NT₅₀ values relative to H1 genotype-elicited serum. For (B), the x-axis indicates the various measles pseudotyped virus genotypes, and the y-axis shows the fold change in NT₅₀ values relative to B3 genotype-elicited serum.

differences at each time point. No significant differences in antibody levels were observed between male and female subjects across all groups (Figure 4A–E).

MMR-vaccinated sera demonstrated average neutralizing titers against genotypes A, H1, B3, D4, D8, D9, D11, and G3 of 3,929; 6,330; 4,046; 7,482; 5,373; 3,575; 2,241; and 8,390, respectively. The lowest neutralization titer was observed against genotype D11, with only a 1.8-fold difference compared to other genotypes, indicating that the current vaccine confers protective immunity against diverse circulating measles virus strains (Figure 4F).

Antibody Levels in Adults

To assess measles virus antibody levels in the general population, we performed the pseudotyped virus neutralization assay on 50 adult serum samples. The geometric mean neutralizing antibody titer among adults was 1,322, with 12% (6/50) of sera falling below the detection threshold, highlighting the need to strengthen herd immunity. When samples were stratified by age and sex, Duncan's Multiple Range Test revealed no significant differences in measles antibody levels among the adult cohorts (Figure 5).

DISCUSSION

Measles is recognized as one of the most important targets for global eradication due to the high efficacy and widespread availability of the measles vaccine, combined with the virus having a single serotype and no animal reservoir (7). The core strategy for measles control and elimination involves establishing and

maintaining herd immunity through high vaccine coverage, thereby interrupting viral transmission and reducing measles-related mortality. In recent years, global health organizations have achieved significant progress in expanding measles vaccination coverage and controlling outbreaks through sustained efforts. However, in certain countries and regions, factors including vaccine hesitancy, insufficient healthcare infrastructure, and socioeconomic challenges have contributed to declining vaccination rates. Suboptimal vaccine coverage has resulted in measles resurgence and outbreaks, including the reestablishment of endemic transmission in countries where measles had previously been eliminated (8). Between 2022 and 2023, the estimated number of global measles cases increased by 20%. In 2023, 57 countries experienced large-scale or disruptive measles outbreaks, defined by the IA2030 global monitoring framework as ≥20 cases per million inhabitants, representing a 58% increase in affected countries compared to 2022. Among these countries, 47% (27 outbreaks) occurred in the African region, 23% (13 outbreaks) in the Eastern Mediterranean region, 18% (10 outbreaks) in the European region, 7% (4 outbreaks) in the Western Pacific region, and 5% (3 outbreaks) in the Americas (9). With progress in global measles elimination efforts, the diversity of circulating strains has declined substantially. Genotypes D11, B2, G3, D9, H1, and D4 were last detected in 2010, 2011, 2014, 2019, 2019, and 2020, respectively (10). Currently, only genotypes B3 and D8 remain endemic, exhibiting distinct regional distributions: B3 predominates in Africa, the Americas, and the Eastern Mediterranean, whereas D8 represents the main genotype in Europe, Southeast Asia, and the

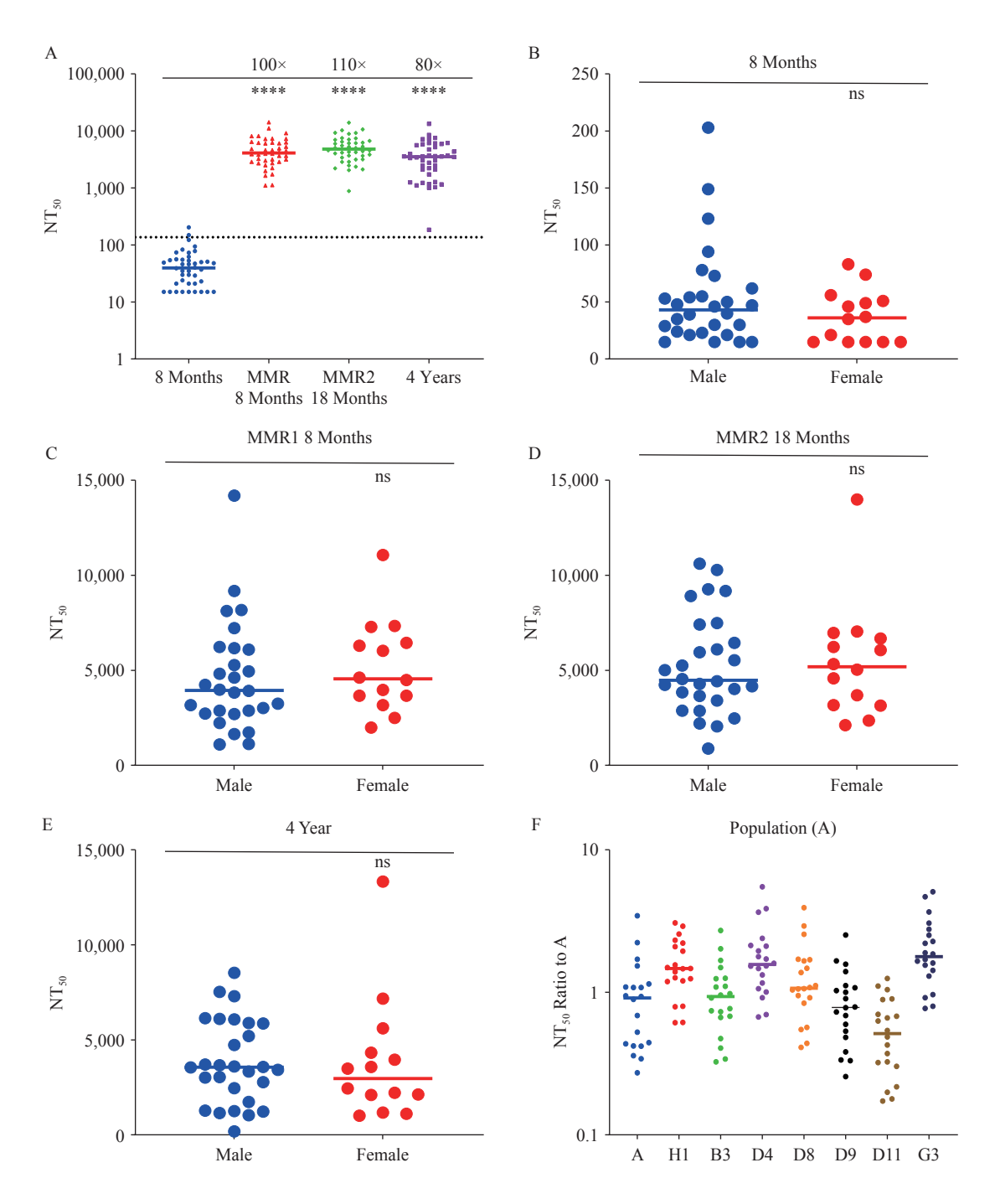


FIGURE 4. Determination of vaccine-induced measles antibody levels. (A) Overall measles neutralizing antibody levels in infant sera across vaccination time points. (B) Pre-vaccination measles antibody levels stratified by sex. (C) Post-first-dose measles antibody levels stratified by sex. (D) Post-second-dose measles antibody levels stratified by sex. (E) Measles antibody levels in 4-year-old children stratified by sex. (F) Cross-neutralization of measles pseudotyped viruses representing diverse genotypes by vaccinated sera.

Note: ns means no significant difference. For (A), the x-axis represents four groups based on serum collection timing: pre-MMR vaccination (8 months), post-first dose (8 months), post-second dose (18 months), and at 4 years of age. The y-axis displays NT_{50} values. Duncan's Multiple Range Test was applied for group comparisons. For (B), The x-axis distinguishes male and female groups, while the y-axis represents NT_{50} values; Student's *t*-test was performed. For (C, D, and E), the x-axis distinguishes male and female groups, while the y-axis represents NT_{50} values; Student's *t*-test was performed. For (F), The x-axis indicates measles pseudotyped virus genotypes, and the y-axis displays relative NT_{50} values normalized to the vaccine strain (genotype A).

Abbreviation: NT_{50} =50% neutralizing antibody titer. **** P<0.001.

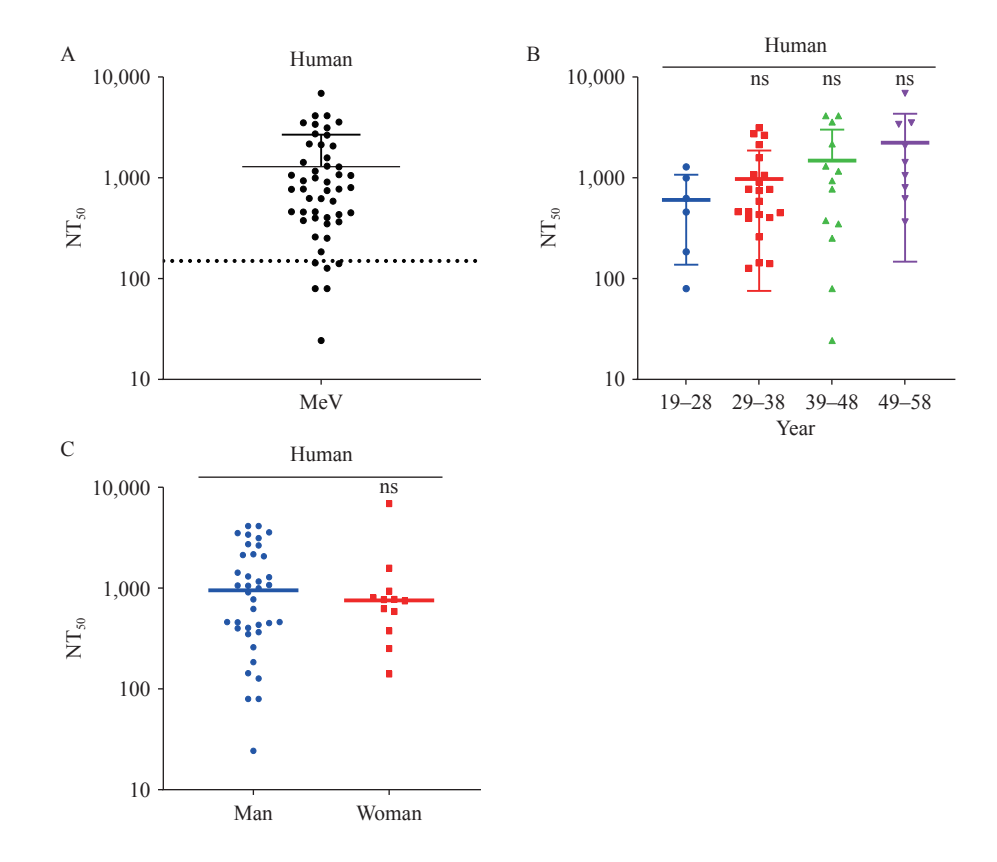


FIGURE 5. Detection of serum measles antibody levels in adults. (A) Overall measles neutralizing antibody levels in adult sera. The y-axis indicates NT50 values. (B) Measles antibody levels in adult sera stratified by age. (C) Measles antibody levels in adult sera stratified by sex.

Note: ns means no significant difference. For (A), the 50 adult samples were divided into five age groups spanning 10 years each (19–28, 29–38, 39–48, and 49–58 years). The y-axis indicates NT50 values; Duncan's Multiple Range Test was performed among groups. For (C), the y-axis indicates NT50 values; Student's t-test was performed. Abbreviation: NT50=50% neutralizing antibody titer.

Western Pacific (Supplementary Figure S3, available at https://weekly.chinacdc.cn/).

Our study demonstrated that immune sera elicited by measles virus genotypes H1 and B3 exhibited robust cross-NT₅₀ against the other seven genotypes, with not exceeding 6.4-fold and differences consistently maintained above 150. These findings demonstrate significant cross-neutralization among different genotypes and indicate that current vaccines provide effective protection against all circulating strains. The regional distribution of genotypes is therefore not attributed to immune escape but is primarily associated with low vaccination coverage and the susceptibility of individuals or populations lacking neutralizing antibodies. Previous research has suggested that the epitope recognized by MAb-BH26 represents the most important immunodominant epitope, as MAb-BH26 inhibits the binding of approximately 60% of human serum antibodies in both convalescent measles patients and vaccinees (11). The binding site of MAb-BH26 is predicted to reside within either the

amino acid region 571-579 or 190-200, with both potentially contributing recognition. Notably, the residues at positions 191–195 are located in close proximity to the receptorbinding site (RBS) and interact directly with SLAM (12). These residues are 100% conserved across all eight strains tested in our study. Furthermore, amino acids 379-400 have been identified as forming an immunodominant epitope known hemagglutinating and noose epitope (HNE) (13). The cysteines at positions 386 and 394 are critical for maintaining its conformational integrity. Among the strains examined in our study, cysteines at positions 386 and 394 are completely conserved, with only variations occurring in other residues. Therefore, the high sequence conservation at these immunodominant sites likely explains the absence of immune escape among circulating measles virus genotypes.

We established the cut-off value for neutralization assays using pre-vaccination sera from 8-month-old

infants as negative controls (14). Compared to prevaccination baseline levels, measles antibody titers increased approximately 100-fold and 110-fold after the first and second doses of the MMR vaccine, respectively, demonstrating strong immunogenicity. At 4 years of age, antibody levels remained elevated, approximately 80-fold higher than pre-vaccination levels, indicating durable immunity. Additionally, neutralization assays performed with 50 adult plasma samples revealed residual antibody levels 28-fold higher than those observed in pre-vaccination infant sera. However, only 88% (44/50) of adult sera exhibited antibody titers above the detection threshold, highlighting the risk of susceptible individuals accumulating in the population and underscoring the critical need to strengthen herd immunity. These findings are consistent with research conducted by Minghao Zhou's team (15).

These findings demonstrate that regions and countries where measles has not been fully eliminated must accelerate efforts to increase vaccine coverage and ensure broader population immunity for achieving herd protection. Furthermore, enhanced surveillance and reporting systems are essential for the prompt detection and control of outbreaks. In countries and regions where measles has been successfully eliminated, continued vigilance through active monitoring and rapid response measures remains critical to prevent disease resurgence.

In summary, this study establishes a rapid, safe, convenient, automatable, and standardized *in vitro* neutralization assay utilizing pseudotyped measles virus. This assay can be effectively applied to monitor antibody levels in susceptible populations and evaluate vaccine immunogenicity. The method holds significant promise for large-scale, population-wide antibody surveillance, which will facilitate the assessment of measles epidemiology, outbreak risk prediction, and acceleration of global measles elimination efforts.

Ethical statement: Pathogen testing for infants and young children approval by the Medical Ethics Committee of the Shandong Provincial Center for Disease Control and Prevention [SDJK(K)2024-053-01]. Mouse experiments were conducted under approval from the Institutional Animal Care and Use Committee at the National Institutes for Food and Drug Control (NIFDC) [2024(B)048]. Human serum samples were collected with informed consent for pathogen marker detection.

Conflicts of interest: No conflicts of interest.

Funding: Supported by the Major Project of

Guangzhou National Laboratory, Grant No. GZNL2024A01019.

doi: 10.46234/ccdcw2025.224

* Corresponding authors: Juan Li, lijuan@nifdc.org.cn; Suting Wang, sdsjbyfkzzx-mys@shandong.cn; Yan Zhang, zhangyan@ivdc.chinacdc.cn.

Copyright © 2025 by Chinese Center for Disease Control and Prevention. All content is distributed under a Creative Commons Attribution Non Commercial License 4.0 (CC BY-NC).

Submitted: July 22, 2025 Accepted: September 25, 2025 Issued: October 17, 2025

REFERENCES

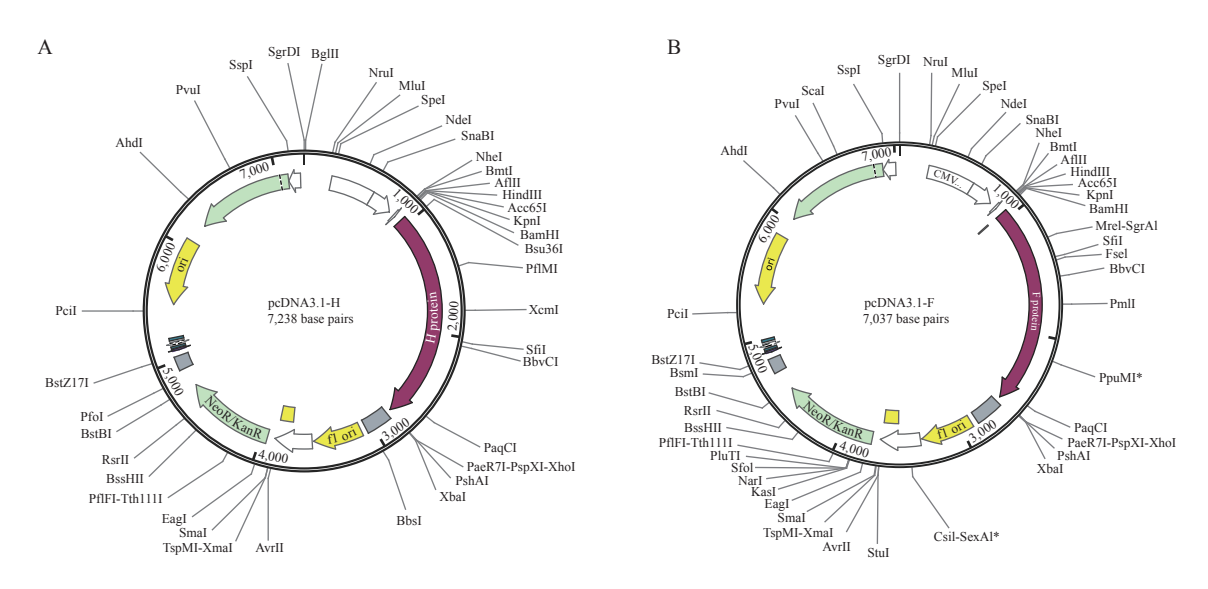
- Moss WJ. Measles. Lancet 2017;390(10111):2490 502. https://doi. org/10.1016/S0140-6736(17)31463-0.
- Ikegame S, Hashiguchi T, Hung CT, Dobrindt K, Brennand KJ, Takeda M, et al. Fitness selection of hyperfusogenic measles virus F proteins associated with neuropathogenic phenotypes. Proc Natl Acad Sci USA 2021;118(18):e2026027118. https://doi.org/10.1073/pnas. 2026027118.
- Bidari S, Yang W. Global resurgence of measles in the vaccination era and influencing factors. Int J Infect Dis 2024;147:107189. https://doi. org/10.1016/j.ijid.2024.107189.
- WHO. Measles United States of America. 2025. https://www.who. int/emergencies/disease-outbreak-news/item/2025-DON561. [2025-3-27]
- Lutz CS, Hasan AZ, Bolotin S, Crowcroft NS, Cutts FT, Joh E, et al. Comparison of measles IgG enzyme immunoassays (EIA) versus plaque reduction neutralization test (PRNT) for measuring measles serostatus: a systematic review of head-to-head analyses of measles IgG EIA and PRNT. BMC Infect Dis 2023;23(1):367. https://doi.org/10.1186/ s12879-023-08199-8.
- Liang ZT, Wu X, Wu JJ, Liu S, Tong JC, Li T, et al. Development of an automated, high-throughput SARS-CoV-2 neutralization assay based on a pseudotyped virus using a vesicular stomatitis virus (VSV) vector. Emerg Microbes Infect 2023;12(2):e2261566. https://doi.org/10.1080/ 22221751.2023.2261566.
- Rota PA, Moss WJ, Takeda M, de Swart RL, Thompson KM, Goodson JL. Measles. Nat Rev Dis Primers 2016;2(1):16049. https://doi.org/10. 1038/nrdp.2016.49.
- Tahir IM, Kumar V, Faisal H, Gill A, Kumari V, Tahir HM, et al. Contagion comeback: unravelling the measles outbreak across the USA. Front Public Health 2024;12:1491927. https://doi.org/10.3389/fpubl. 2024 1491927
- 9. Minta AA, Ferrari M, Antoni S, Lambert B, Sayi TS, Hsu CH, et al.

¹ Division of HIV/AIDS and Sexually Transmitted Virus Vaccines, Institute for Biological Product Control, State Key Laboratory of Drug Regulatory Science, National Institutes for Food and Drug Control (NIFDC), Beijing, China; ² WHO Western Pacific Regional Measles/Rubella Reference Laboratory, National Key Laboratory for Intelligent Tracking and Forecasting of Infectious Diseases, NHC Key Laboratory of Medical Virology and Viral Diseases, National Institute for Viral Disease Control and Prevention, Chinese Center for Disease Control and Prevention, Beijing, China; ³ Department of Research & Development, Taibang Biologics Group, Beijing, China; ⁴ Institute of Medical Biology, Chinese Academy of Medical Sciences, Kunming City, Yunnan Province, China; ⁵ Division of Respiratory Virus Vaccines, National Institutes for Food and Drug Control, Beijing, China; ⁶ Shandong Center for Disease Control and Prevention, Jinan City, Shandong Province, China.

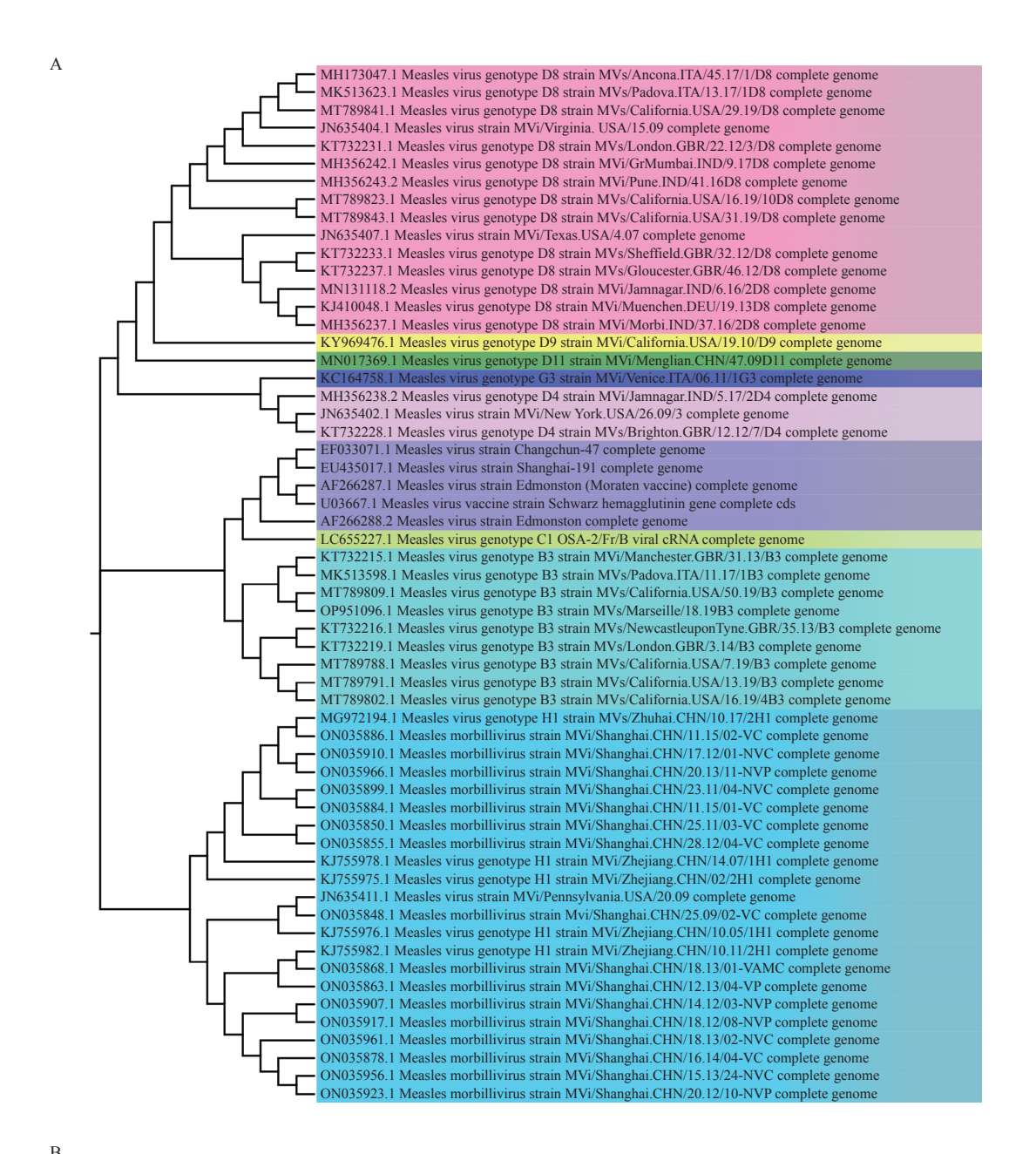
China CDC Weekly

- Progress toward measles elimination worldwide, 2000–2023. MMWR Morb Mortal Wkly Rep 2024;73(45):1036 42. https://doi.org/10.15585/mmwr.mm7345a4.
- Bankamp B, Kim G, Hart D, Beck A, Ben Mamou M, Penedos A, et al. Global update on measles molecular epidemiology. Vaccines 2024;12 (7):810. https://doi.org/10.3390/vaccines12070810.
- 11. Ertl OT, Wenz DC, Bouche FB, Berbers GAM, Muller CP. Immunodominant domains of the Measles virus hemagglutinin protein eliciting a neutralizing human B cell response. Arch Virol 2003;148(11):2195 206. https://doi.org/10.1007/s00705-003-0159-9.
- Hashiguchi T, Ose T, Kubota M, Maita N, Kamishikiryo J, Maenaka K, et al. Structure of the measles virus hemagglutinin bound to its cellular receptor SLAM. Nat Struct Mol Biol 2011;18(2):135 41. https://doi.org/10.1038/nsmb.1969.
- Ziegler D, Fournier P, Berbers GAH, Steuer H, Wiesmüller KH, Fleckenstein B, et al. Protection against measles virus encephalitis by monoclonal antibodies binding to a cystine loop domain of the H protein mimicked by peptides which are not recognized by maternal antibodies. J Gen Virol 1996;77(10):2479 – 89. https://doi.org/10. 1099/0022-1317-77-10-2479.
- 14. Wang QL, Wang W, Winter AK, Zhan ZF, Ajelli M, Trentini F, et al. Long-term measles antibody profiles following different vaccine schedules in China, a longitudinal study. Nat Commun 2023;14(1): 1746. https://doi.org/10.1038/s41467-023-37407-x.
- Hu Y, Lu PS, Deng XY, Guo HX, Zhou MH. The declining antibody level of measles virus in China population, 2009-2015. BMC Public Health 2018;18(1):906. https://doi.org/10.1186/s12889-018-5759-0.

SUPPLEMENTARY MATERIAL



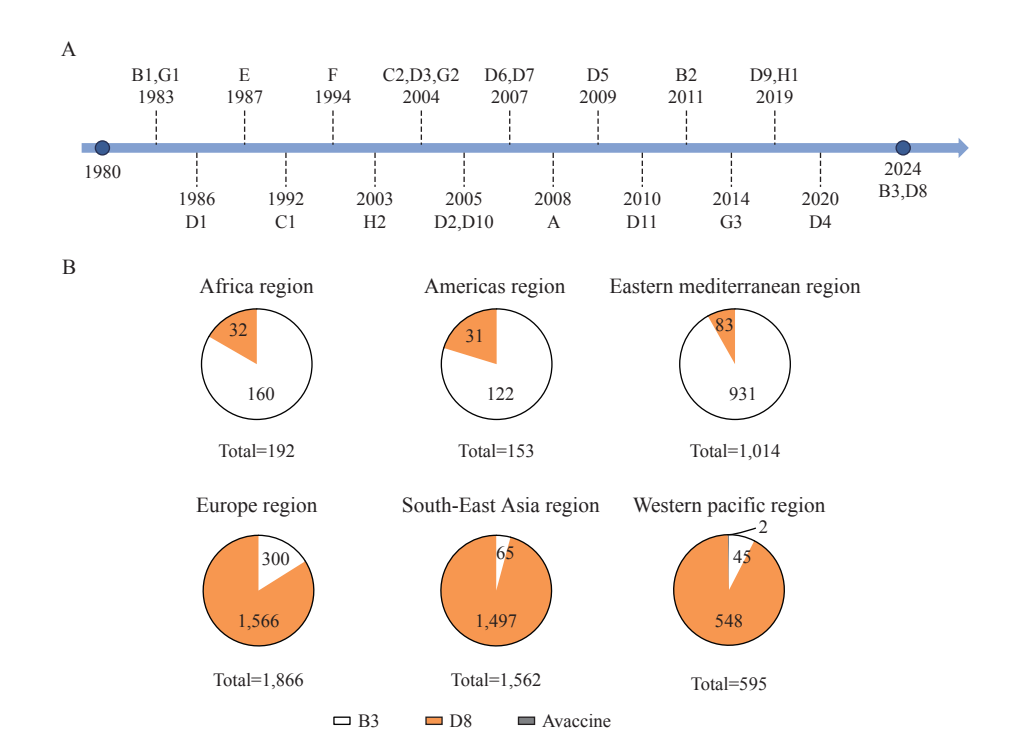
SUPPLEMENTARY FIGURE S1. Vector maps of expression plasmids. (A) Vector map of plasmid pcDNA3.1-H. (B) Vector map of plasmid pcDNA3.1-F.



NSPORDR | NAFYKONPHEKGSR | V | NREHLM | DRPYYLLAYLFVMFLSL | GLLA | AG | RLHRAA! YTAE | HKSLSTNLDVTNS | EHQVKDVLTPLFK | | GDEVGLRTPQRFTDLVKE | SDK | KFLNPDREYDFRDLTWC | NPPER | KLDYDQYCADVAAEELMNALVNSTLLEABATVQFLAVSKGNCSGPTT | RGQFSN | NSLSLLDLYLSBGYNVSS | YTMTSQGNYGGTYLVEKPNLSKGSELSQLSMARVFEVGY | RNPGLGAPVFHWTNYFEQPYSADESNCWVALGELKEAALC | HSEDS | T | PYQGSGKGVSFQLVKLGVWKSPTDMQSWVPLSTDDPY | DRLYLSSHBGV | ADNQAKWAYPTTRTDDKLRMETCFQQACKGK | QALCENEEWAPLKDNR | PSYGYLSVBLSLTYELK | K | ASGFGPL | THGSGNDLYKSNENNAYWLT | PPMKNLALGV | NTLEW | PREKVSP-LFTVP | KEAGEDCHAPTYLPAEVDGDVKLSSNLV | LPGQDLQYVLATYDTSRVEHAVVYYVYSPSRSFSYFYPFRLP | KGYP | ELQVECFTVDQKLWCRHFCVLADSESGGH | THSGNV GNGVSCTXTREDGTNRR

SUPPLEMENTARY FIGURE S2. Measles virus H protein sequence analysis. (A) Phylogenetic tree constructed using nucleotide sequences of the H protein from 58 measles virus strains. (B) Amino acid sequence analysis of the H protein from eight selected measles virus strains.

China CDC Weekly



SUPPLEMENTARY FIGURE S3. Global distribution and temporal trends of measles virus genotypes. (A) Most recent detection year for each of the 24 measles virus genotypes documented in the MeaNS database. (B) Geographic circulation patterns of measles virus genotypes between January 2022 and December 2023. Note: Data source are MeaNS2 database (Genotypes).